A SIMPLE MODEL OF SOFT X-RAY PHOTOEMISSION

R. R. Schaefer

November 1971

R&D Associates

POST OFFICE BOX 3580
SANTA MONICA, CALIFORNIA 90403

525 WILSHIRE BOULEVARD
TELEPHONE: (213) 451-5838

RDA-TR-036-DNA

A SIMPLE MODEL OF SOFT X-RAY PHOTOEMISSION

By

R. R. Schaefer

November 1971

UNCLASSIFIED

Security Classification

I

DOCUMENT CONTROL DATA - R & D

(Security classification of title, body of abstract and indexing annotation must be entered when the overall report is classified)

1. ORIGINATING ACTIVITY (Corporate author)	2a. REPORT SECURITY CLASSIFICATION
R&D Associates P.O. Box 3580 Santa Monica, California 90403	UNCLASSIFIED 2b. GROUP

3. REPORT TITLE

A SIMPLE MODEL OF SOFT X-RAY PHOTOEMISSION

4. DESCRIPTIVE NOTES *(Type of report and inclusive dates)*

5. AUTHOR(S) *(First name, middle initial, last name)*

Richard R. Schaefer

6. REPORT DATE	7a. TOTAL NO. OF PAGES	7b. NO. OF REFS
November 1971	19	8

8a. CONTRACT OR GRANT NO.	9a. ORIGINATOR'S REPORT NUMBER(S)
DASA 01-71-C-0103 b. PROJECT NO.	RDA-TR-036-DNA
c.	9b. OTHER REPORT NO(S) *(Any other numbers that may be assigned this report)*
d.	

10. DISTRIBUTION STATEMENT

11. SUPPLEMENTARY NOTES	12. SPONSORING MILITARY ACTIVITY

13. ABSTRACT

In order to evaluate some of the features of the electromagnetic response of space systems to pulsed, plane wave photon environments, it is necessary to understand the intensity, energy spectrum, and angular distribution of the electron emission current: For a realistic application, the electron emission spectrum and angular distribution can be found by convolving the incident photon spectrum with the electron yield as a function of photon energy. This electron yield, which expresses the number of electrons emitted from a surface per incident photon, can be expected to vary with angle of photon incidence and material composition as well as with photon energy. (U)

Soft x-rays contribute to electron emission primarily through photoelectric interactions and the electron yield for soft x-rays will be referred to here as the photoelectric yield. In this paper, a simple model of the photoelectric yield is proposed and predictions based upon the model are compared with published experimental data. Furthermore, simple expressions for the electron emission current for arbitrary incident photon fluxes are derived for the higher energy electron components. (U)

DD FORM 1 NOV 68 1473 REPLACES DD FORM 1473, 1 JAN 64, WHICH IS OBSOLETE FOR ARMY USE.

UNCLASSIFIED

PREFACE

This report describes results of an investigation into the feasibility of predicting photoelectric yields on the basis of a simple model.

It has been determined that the quantum yield, yield spectrum, and angle of photon incidence dependence are easily predicted on the basis of the proposed model. It is further suspected but as yet unsubstantiated that the angle of electron emission distribution is also adequately expressed by the model. The difference between forward and backward yield is not accounted for in the proposed model but it is suggested that this difference can be expressed in terms of anistropy factors determined via experiments or Monte Carlo calculations.

The value of the proposed model is that it represents, in effect, a curve fit to the experimental and Monte Carlo data, and a scheme for extrapolation or interpolation to regions in which data is not available. Thus, the simple formulas developed here can be used to bridge the gap between the more detailed investigations and the user community.

ABSTRACT

A simple model of the photoelectric yield is proposed and predictions of the yield and yield spectrum based upon this model are compared with published experimental data for aluminum. Furthermore, simple expressions for the electron emission current for arbitrary incident photon fluxes are derived for the higher energy components of the photoelectric yield. Since the photoelectrons are assumed to propagate isotropically, no distinction is made between forward and backscatter yields or emission currents.

CONTENTS

PREFACE ii

ABSTRACT iii

Section

I. INTRODUCTION 1

II. A PHOTOELECTRIC YIELD MODEL 1

III. PREDICTION OF PHOTOELECTRIC YIELD AND COMPARISON WITH EXPERIMENTAL DATA FOR ALUMINUM 8

IV. THE PHOTOELECTRIC EMISSION CURRENT FOR AN ARBITRARY INCIDENT PHOTON FLUX 15

REFERENCES 18

I. INTRODUCTION

In order to evaluate some of the features of the electromagnetic response of systems to pulsed, photon environments, it is necessary to understand the intensity, energy spectrum, and angular distribution of the electron emission current. For a realistic application, the electron emission spectrum and angular distribution can be found by convolving the incident photon spectrum with the electron yield as a function of photon energy. This electron yield, which expresses the number of electrons emitted from a surface per incident photon, can be expected to vary with angle of photon incidence and material composition as well as with photon energy.

Soft* x-rays contribute to electron emission primarily through photoelectric interactions and the electron yield for soft x-rays will be referred to here as the photoelectric yield. In this paper a simple model of the photoelectric yield is proposed and predictions based upon the model are compared with published experimental data. Furthermore, simple expressions for the electron emission current for arbitrary incident photon fluxes are derived for the higher energy electron components.

II. A PHOTOELECTRIC YIELD MODEL

The total photoelectric yield receives contributions from primary photoelectrons, Auger electrons, and secondary electrons (also referred to as "knock-on" electrons or delta rays). The photoelectric yield model proposed here consists of assuming that, for each component

1. The electrons are initiated with uniform density in the

---

* The term "soft" x-ray will be interpreted here to include all x-rays which are more apt to undergo photoelectric than Compton collisions, and hence the energy range will vary with material. For aluminum, x-rays below 50 KeV can be considered "soft".

struck material, with the primary and Auger sources densities equal to $\phi\mu_{p.e.}/\cos\alpha$ where ϕ is the photon flux at the surface, $\mu_{p.e.}$ is the mass absorption coefficient, and α is the angle of incidence of the photon with respect to the normal to the surface.

2. The electrons propagate isotropically from their point of initiation.
3. The electrons travel precisely their mean forward range (a function of the electron energy which is a function of the incident photon energy, $h\nu$, and the atomic electron binding energies) in straight paths.
4. The electrons lose energy continuously according to an effective stopping power which is just the ordinary stopping power times the continuous slowing down approximation range divided by the mean forward range.*

The first assumption, that the electron source is uniform, is reasonable for homogeneous materials since electrons are emitted only from within a few electron ranges of the surface and except for extremely acute angles of incidence, the photon flux does not attenuate appreciably within a few electron ranges. The next assumption, that the electrons propagate isotropically from their point of initiation is reasonable for purposes of estimating the emission spectrum and angular distribution because of the randomizing effects of multiple electron collisions. The difference between forward and backward emission is lost in this assumption, however. The third assumption, that the electrons travel in straight paths precisely their mean forward range, is unjustifiable except from the standpoint that it is convenient analytically and at least does not

---

* Electron transmission curves observed in numerous experiments [1] as well as in Monte Carlo electron transport calculations indicate that the mean forward range of electrons is roughly half of the maximum range predicted on the basis of the continuous slowing down approximation [4]. Therefore, an effective stopping power equal to twice the ordinary stopping power [4] is assumed in the following pages.

affect the total photoelectric yield (integrated over exit angle and energy) which is proportional to the mean forward range. Finally, the assumption that electrons lose energy continuously according to an effective stopping power is also unjustifiable except that it is compatible with the third assumption, it is convenient to use, and results in photoelectric yield spectra that agree surprisingly well with measured spectra.

With this model in mind and with reference to Figure 1, we can express the primary electron contributions to the photoelectric yield, Y, coming from a unit volume at a slant depth, r, and angle, θ, as

$$\frac{dY_i}{dv} = \frac{\mu_i(h\nu)\ \cos\theta}{\cos\alpha \cdot 4\pi r^2} \tag{1}$$

where r is the slant depth at which the electrons are born,
θ is the electron exit angle with respect to the normal to the surface,
α is the angle of photon incidence with respect to the normal to the surface,
$h\nu$ is the incident photon energy, and,
$\mu_i(h\nu)$ is the mass absorption coefficient (cm^2/gm) at $h\nu$ due to interaction with the i^{th} electron shell

And since $dv = 2\pi r^2 \sin\theta\, d\theta\, dr$ we can express the yield as

$$\frac{d^2Y_i}{dr\,d\theta} = \frac{\mu_i(h\nu)\cos\theta\sin\theta}{2 \cdot \cos\alpha} \tag{2}$$

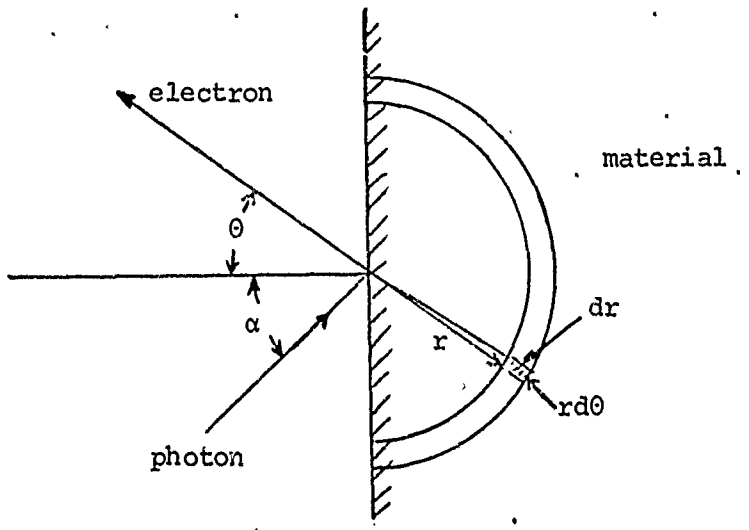

Figure 1. The Photoelectric Yield Model Geometry

Furthermore, given dE/dr, the effective electron stopping power, the electron exit energy and angular distribution can be expressed as

$$\frac{d^2Y_i}{dEd\Theta} = \frac{d^2Y_i}{drd\Theta} \Big/ \frac{dE}{dr} \left(\frac{\text{electrons/photon}}{\text{unit energy - unit angle}} \right)$$

$$= \frac{\mu_i(h\nu)\ \cos\Theta\sin\Theta}{2\ \cos\alpha} \Big/ \frac{dE}{dr} \qquad (3)$$

for $0 < E < h\nu - E_i$, where E_i is the binding energy of the i^{th} electron shell.

One interesting observation that can be made on the basis of Equation (3) is that the angle and energy dependences are separate. The angular distribution is identical for each energy component and the energy distribution is independent of electron exit angle. Furthermore, the average

and most probable exit angle is 45°. If expressed in terms of electrons per steradian the familiar cosine distribution emerges. Although Equation (3) applies to primary electrons, the same angle and energy dependence features apply to Auger and secondary electron components of the photoelectric yield.

Integration of Equation (3) over angle results in the primary electron energy spectrum

$$\frac{dY_i}{dE} = \frac{\mu_i(h\nu)}{4\cos\alpha} \Big/ \frac{dE}{dr} \tag{4}$$

Further integration over electron energy results in the primary electron yield from the i^{th} shell

$$Y_i(h\nu) = \int_0^{h\nu - E_i} dY_i/dE \; dE$$

$$= \frac{\mu_i(h\nu)\,\bar{R}(h\nu - E_i)}{4\cos\alpha} \tag{5}$$

where $\bar{R}$ is the mean forward electron range.

The Auger electron component results from outer shell electrons falling into an inner shell and the energy difference being transferred to an outer shell electron. A dominant component of the Auger emission for photons above the K edge energy is driven by K shell excitation in which case an L shell electron receives $E_K - 2E_L$ as kinetic energy where E_K is the K shell energy and E_L is the L shell energy The Auger effect, also referred to as auto-ionization, competes with fluorescence. The probability of fluorescence, p(f), resulting from decay to the K shell is [2]

$$p(f) = z^4/(z^4 + 33^4) \tag{6}$$

where z is the atomic number.

The probability of auto-ionization, p(a), is just

$$p(a) = 1 - p(f)$$

$$= 1 - z^4/(z^4 + 33^4) \tag{7}$$

thus, for low z materials, auto-ionization is very probable (when permissible).

The K shell Auger or auto-ionization component of the photoelectric yield, Y_a, can be expressed as

$$\frac{d^2Y_a(h\nu)}{dEd\theta} = \frac{\mu_K(h\nu)\ \sin\theta\cos\theta}{2\ \cos\alpha} \cdot p(a)/(dE/dr) \tag{8}$$

for $0 < E < E_K - 2E_L$, since the L to K Auger transition is most probable.

The corresponding K shell Auger spectrum $\frac{\partial Y_a}{\partial E}$, is

$$\frac{\partial Y_a}{\partial E} = \frac{\mu_K(h\nu)p(a)}{4\ \cos\alpha} \Big/ (dE/dr) \tag{9}$$

and the total K shell Auger yield, Y_a, is

$$Y_a(h\nu) = \frac{\mu_K(h\nu)p(a)}{4\ \cos\alpha}\ \bar{R}(E_K - 2E_L) \tag{10}$$

Auger electrons arising from decay to the L, M, or N shells can be treated in a similar fashion.

The secondary electron component of the photoelectric yield is the result of collisions of primary and Auger electrons with atomic electrons. The secondary electrons constitute the greater numerical component of the electron emission but do not appreciably augment the higher energy content of the energy spectrum. The secondary electron source is proportional to the flux of higher energy electrons. If $d^2n_s/dE_s dE_p$ is the source of secondary electrons per unit volume per unit secondary electron energy per unit primary electron energy, then

$$\frac{d^2ns}{dE_s dE_p} = \phi_p(E_p)\ p(E_s, E_p) \tag{11}$$

where $\phi_p(E_p)$ is the scalar flux of primary electrons at energy E_p (electrons/unit area - unit energy), and, $p(E_s, E_p)$ is the probability per unit penetration per unit energy of a primary electron with energy E_p producing a secondary electron with energy E_s.

Since the electron flux at the material surface (assuming interface with a vacuum) is half of an isotropic flux and the yield is just one quarter of an isotropic flux

$$\phi_p(E_p) = 2Y_p(E_p) \tag{12}$$

where Y_p is the primary (including Auger) yield.

And finally, the yield of secondary electrons, Y_s, can be expressed as

$$Y_s = \frac{1}{4} \int_0^{h\nu/2} \left[\int_0^{h\nu} 2Y_p(E_p)p(E_s,E_p)dE_p \right] \bar{R}(E_s)dE_s \qquad (13)$$

Higher order secondary electron components of the photoelectric yield due to collisions of these secondary electrons can be modeled by similar analysis. The total photoelectric yield at $h\nu$, $Y(h\nu)$, is just the sum of the primary, Auger, and secondary electron components.

$$Y(h\nu) = \sum_i Y_i + Y_a + Y_s . \qquad (14)$$

The photoelectric yield model developed here suggests that

1. The angular distribution of emitted electrons (per unit angle) is proportional to $\sin\theta\cos\theta$ for all electron energies and all components (primary, Auger, or secondary).
2. The energy spectrum of the photoelectric yield at any angle has the same shape.
3. For thin targets the forward and backward photoelectric yields are identical.*
4. The photoelectric yield and any component thereof increases as the angle of incidence increases toward a grazing incidence according to $(\cos\alpha)^{-1}$, where α is the angle of incidence with respect to the normal at the material surface.

III. PREDICTION OF PHOTOELECTRIC YIELD AND COMPARISON WITH EXPERIMENTAL DATA FOR ALUMINUM

In order to predict the primary and Auger components of photoelectric yield on the basis of Equations (5) and (10), it is necessary to know the mass absorption coefficient versus photon energy and the

* In reality the original anisotropy of the photoelectron source is not completely washed out by scattering and hence differences in forward and backward yield are to be expected. Perhaps these differences (determined by experiment or Monte Carlo calculations) can be expressed in terms of anisotropy factors of functions of $h\nu$.

stopping power versus electron energy. The mass absorption coefficient [3] and electron range power [4] for aluminum are presented in Figure 2. It is assumed in the following predictions that the electron range can be extrapolated as a power of electron energy below 10 KeV.

The resulting K and L shell and Auger components of the yield, together with their sum for normal photon incidence, as computed from Equations (5) and (10), are plotted in Figure 3. Also plotted in Figure 3. is the value of the quantum yield for aluminum observed by Rumsh and Shchemelev [5] for incident CuK_α radiation (8.04 KeV). The quantum yield is defined as the number of acts of electron emission (possibly including multiple electrons) per incident photon. The observed value of .3% for 70° incidence with respect to the normal* corresponds to .1026% for normal incidence. This quantum yield is directly comparable with $Y_K + Y_L$, the sum of the primary photoelectron yields, and as can be seen, the agreement is quite good.

In addition, the total yield for aluminum including secondary electrons as observed by Izrailev [6] and adjusted for incidence angle has been plotted. The difference between this yield and the others is presumably due to the relatively numerous but less energetic secondary electrons counted separately in the Izrailev experiment. The expressions for secondary electron emission suggested in Section II. above have not as yet been evaluated to see to what extent the observed total yield can be predicted. Ganeev and Izrailev [7] note an anomalously high total yield for aluminum which they attribute to the high secondary emission properties of an aluminum oxide film on their sample. The resulting multiplicity of electrons per emission event was observed to be between 6 and 10. Such a multiplicity of electrons accounts for the differences indicated in Figure 3.

---

* Most works on photoelectric yield, including those cited, refer to the angle of incidence as being the angle between the photon path and the surface of the photo cathode and hence the angle of incidence specified in Reference 5 is 20°.

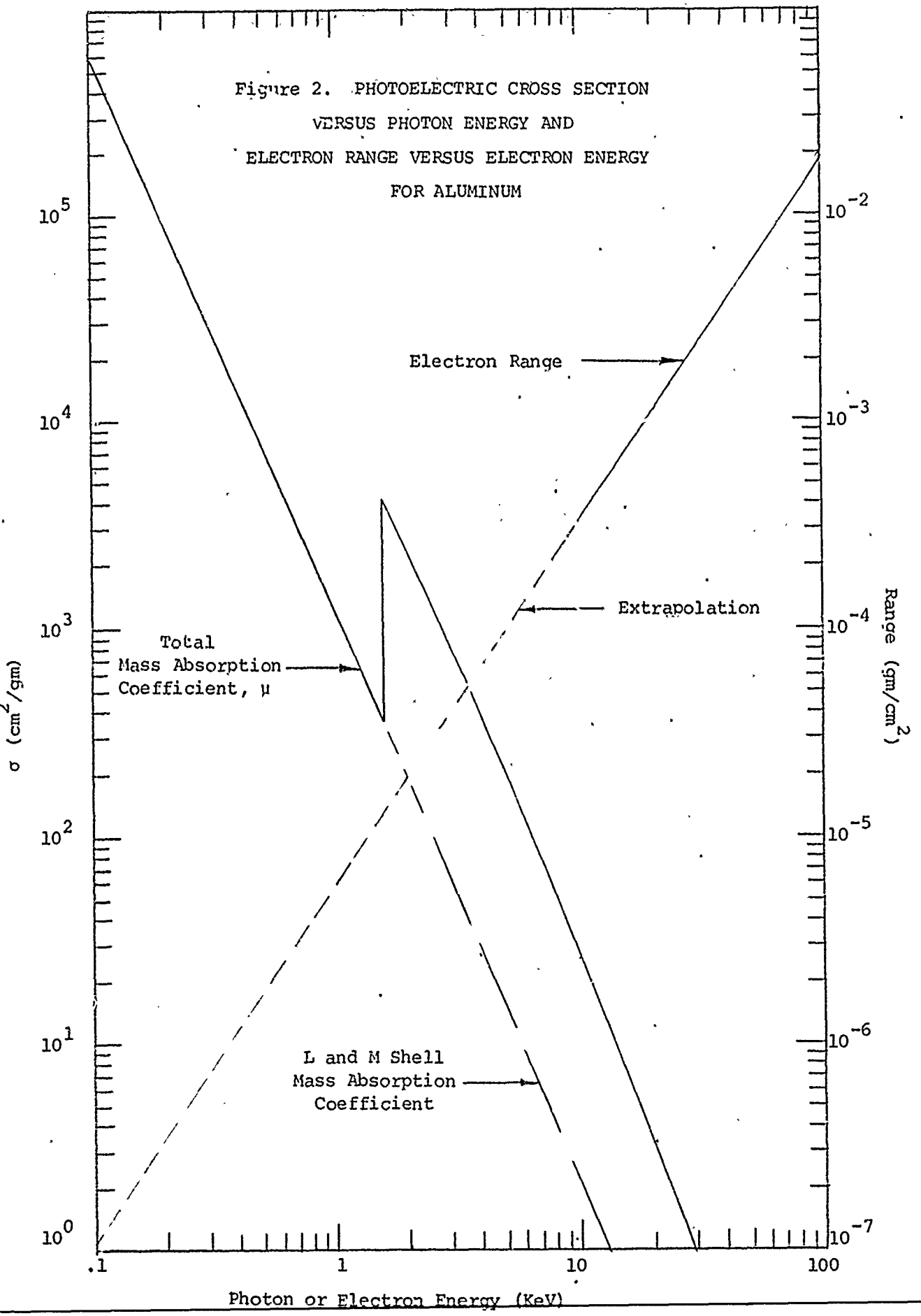

Figure 2. PHOTOELECTRIC CROSS SECTION VERSUS PHOTON ENERGY AND ELECTRON RANGE VERSUS ELECTRON ENERGY FOR ALUMINUM

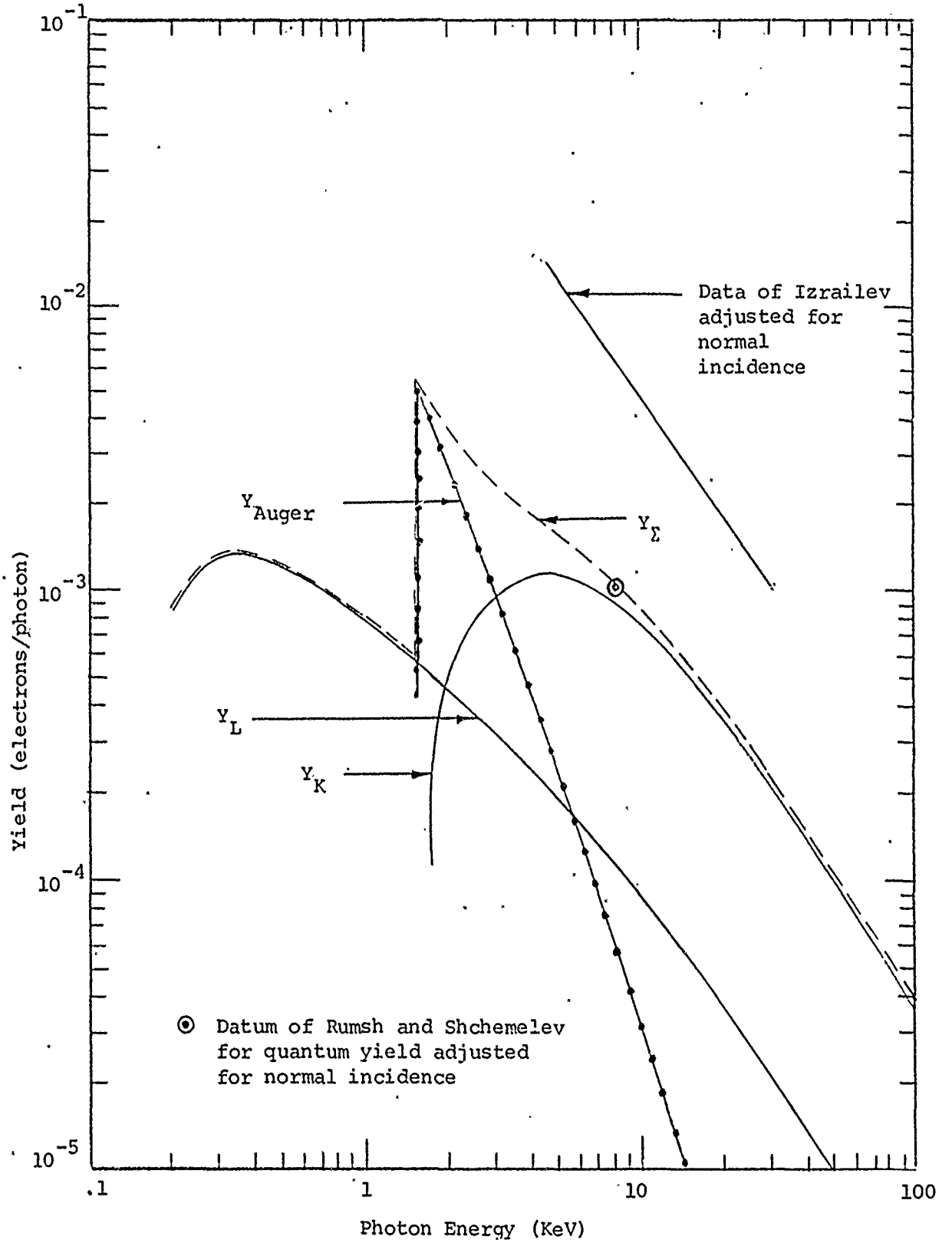

Figure 3. PREDICTED K SHELL, L SHELL, AND AUGER PHOTOELECTRIC YIELDS FOR NORMAL INCIDENCE TOGETHER WITH THEIR SUM Y_Σ OVERLAYED WITH QUANTUM YIELD OF RUMSH AND SHCHEMELEV [5] AND THE TOTAL PHOTOELECTRIC YIELD INCLUDING SECONDARY ELECTRONS AS OBSERVED BY IZRAILEV [6]

In order to examine the energy spectrum of the photoelectric yield according to the proposed model (Equations (4) and (9)) it is necessary to know the effective stopping power, dE/dr. The effective stopping power assumed here is just twice the ordinary electron stopping power [4] which is plotted, for aluminum, in Figure 4. Values of stopping power for electron energies below 10 KeV were obtained by a power law extrapolation from values above 10 KeV. The relative energy spectrum for the photoelectric yield from Aluminum for an incident CuK_α photon source has been reported by Denisov, et. al. [8]. A CuK_α photon source is composed of photons produced following transition of L shell electrons to the K shell in copper, which results in photons with an energy of approximately 8 KeV.

An overlay of a smooth curve through the observed energy spectrum of the photoelectric yield for CuK_α photons incident upon aluminum and the values predicted via Equations (4) and (9) for a normally incident ($\alpha = 0$), 8 KeV photon is presented in Figure 5. The experimental spectrum (with arbitrary units) was scaled to match the prediction at the Auger peak at about 1.4 KeV. This point was chosen for the scaling because it is proportional to the K shell interaction density and hence is not sensitive to the precise incident photon spectrum. Note that both the predicted and observed spectra jump about a factor of two at the maximum Auger electron energy. The agreement of the predicted spectrum with the scaled data would be obtained for any linear relationship between effective and ordinary stopping power.

The fact that the predicted and observed spectra agree in shape so well above 1.4 KeV and that the area under the predicted spectrum agrees with the quantum yield at the same energy (Figure 3.) suggests that the predicted values are fairly accurate in an absolute sense. The flex point in the observed spectrum at about 7.4 KeV can be explained on the basis of K shell photoelectrons from oxygen in the aluminum oxide, Al_2O_3, coating on the aluminum sample. Similarly, components of the observed spectrum between 8 KeV and the predicted L shell yield can be explained on the basis of electrons from higher shells in aluminum and oxygen.

Figure 4. ELECTRON STOPPING POWER VERSUS ELECTRON ENERGY FOR ALUMINUM

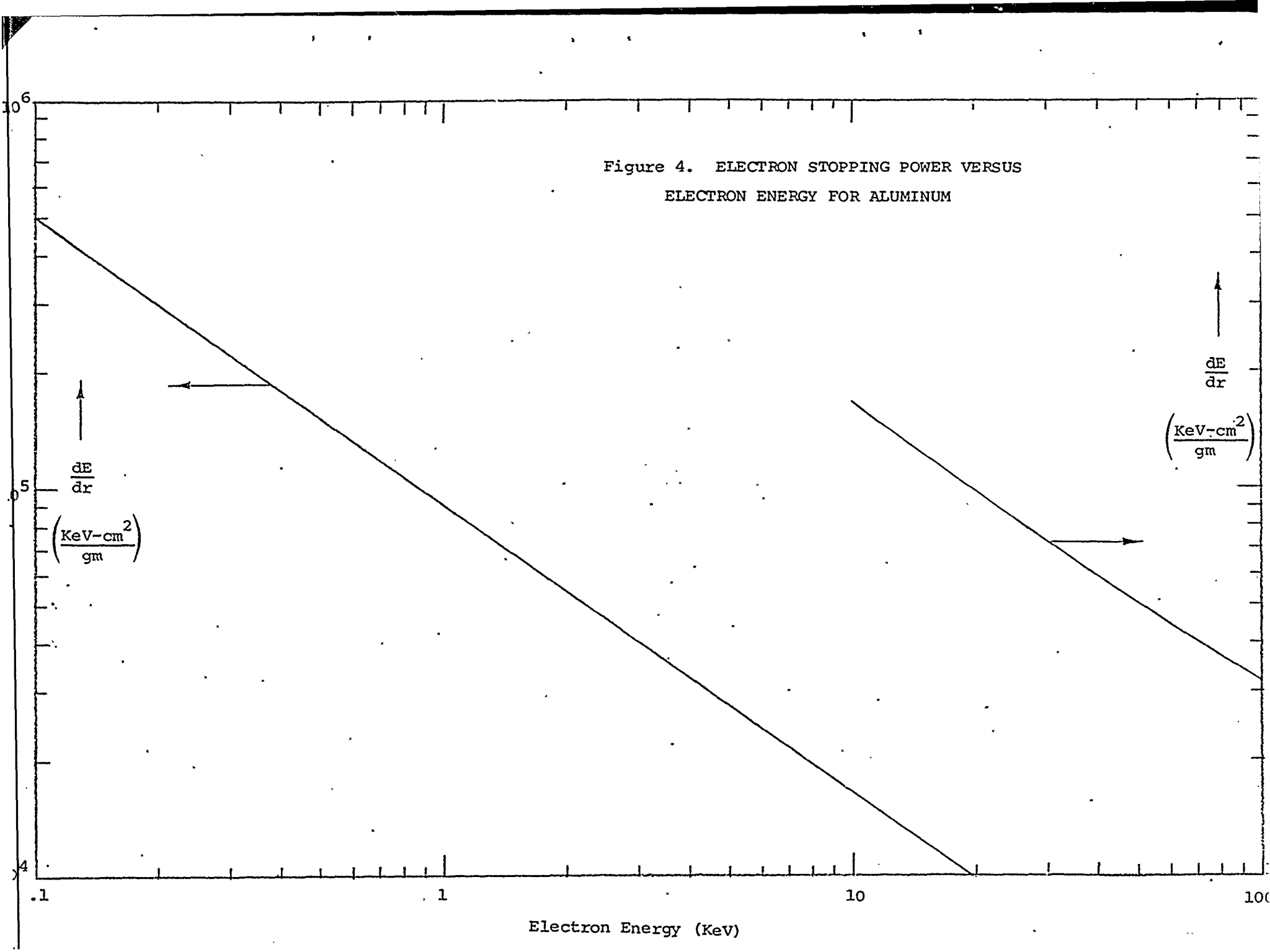

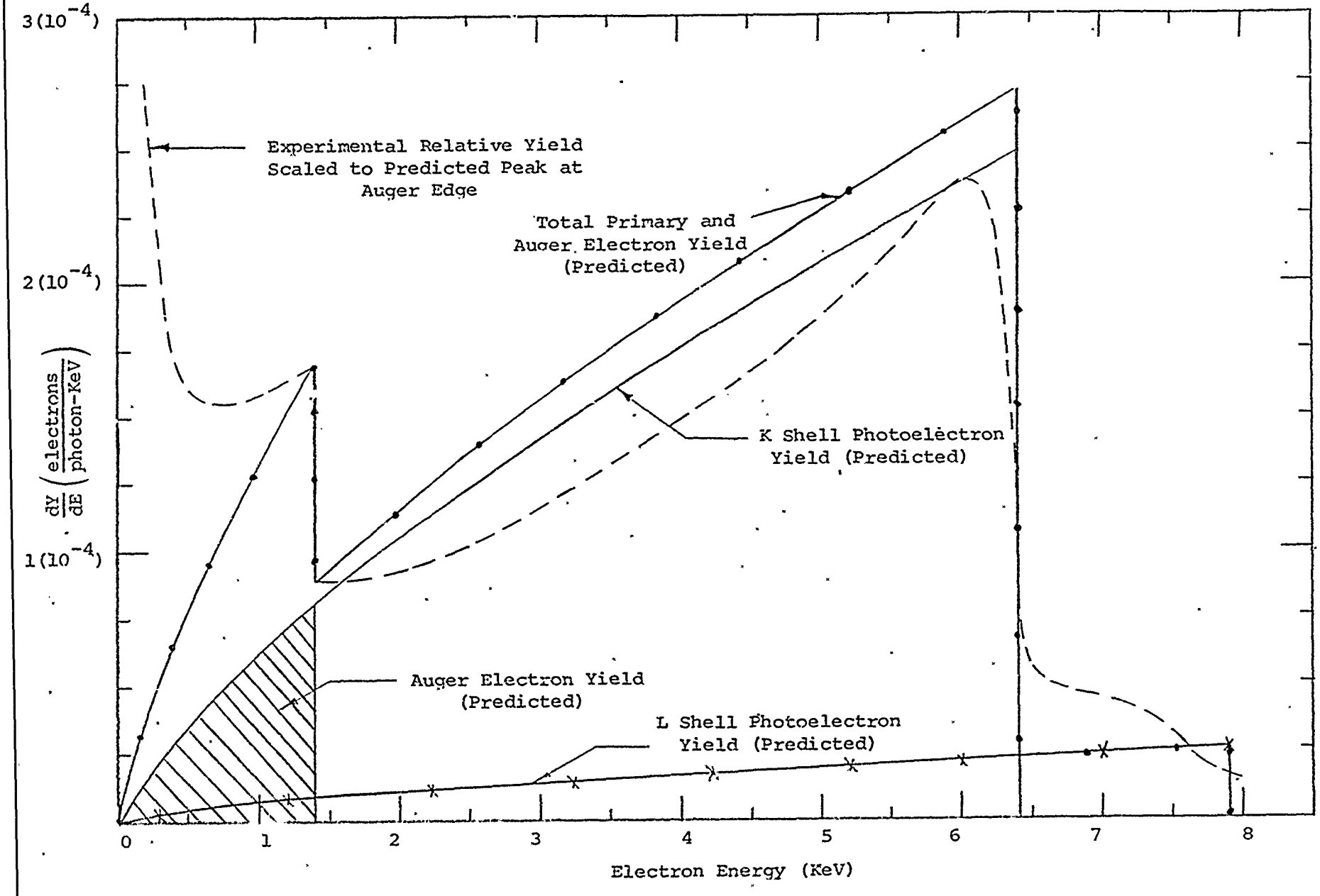

Figure 5. PREDICTED PRIMARY AND AUGER YIELD SPECTRA FOR 8.0 KEV PHOTONS INCIDENT NORMALLY ON ALUMINUM COMPARED WITH EXPERIMENTAL CuK YIELD OBSERVATIONS BY DENISOV, ET AL. [5]

The differences in the spectra at low energies (<1.4 KeV) reflect the absence of secondaries in the predicted yield. The location of the low energy discrepancy allows one to observe that, in this case, the majority of the secondary electrons have energies less than .5 KeV.

IV. THE PHOTOELECTRIC EMISSION CURRENT FOR AN ARBITRARY INCIDENT PHOTON FLUX

Given an arbitrary photon flux incident upon a material surface, the emission current can be expressed in terms of the photoelectric yield. Let $\phi(h\nu,t,\alpha)$ be the number of photons per unit area per unit energy ($h\nu$) per unit time (t) per unit angle (α). Then the electron emission current, $j(E,t,\theta)$ in terms of electrons per unit area per unit energy (E) per unit time (t) per unit angle θ can be expressed as

$$j(E,t,\theta) = \int_{h\nu}\int_{\alpha} \phi(h\nu,t,\alpha)\ \cos\alpha\,(d^2Y/dEd\theta)\,d(h\nu)\,d\alpha \quad * \qquad (15)$$

where Y is the total yield.

Since the emission angle dependence is independent of everything else, it is convenient to let

$$j(E,t,\theta) = j(E,t)p(\theta) \qquad (16)$$

$$\text{where } p(\theta) = 2\sin\theta\cos\theta \qquad (17)$$

and then, integrating out the θ dependence,

---

* It has been assumed that the photon penetration and electron exit times are negligible and hence the emission current bears the same time dependence as the incident flux.

$$j(E,t) = \int_{h\nu} \int_{\alpha} \phi(h\nu,t,\alpha) \cdot \cos\alpha \cdot (dY/dE) \cdot d(h\nu)\,d\alpha \qquad (18)$$

The primary and Auger electron components of the electron emission current can be expressed by letting

$$\frac{dY}{dE} = \sum_i \frac{dY_i}{dE} + \frac{dY_a}{dE} \qquad (19)$$

Conveniently, each of these terms is proportional to $(1/\cos\alpha)$ and hence the emission current is independent of angle of incidence of the photon flux. If we define an incident scalar flux as

$$\phi(h\nu,t) = \int_{\alpha=0}^{\pi/2} \phi(h\nu,t,\alpha)\,d\alpha \qquad (20)$$

then the primary and Auger emission current is just

$$j(E,t) = \left(\frac{dE}{dr}\right)^{-1} \left[\int_{h\nu=E+E_K}^{\infty} \phi(h\nu,t)\,\frac{\mu_K(h\nu)\,dh\nu}{4} + \right.$$

$$\int_{h\nu=E+E_L}^{\infty} \frac{\phi(h\nu,t)\,\mu_L(h\nu)\,dh\nu}{4} + \qquad (21)$$

$$\left. H(E_K-2E_L-E) \cdot p(a) \int_{h\nu=E_K}^{\infty} \phi(h\nu,t)\,\frac{\mu_K(h\nu)\,dh\nu}{4} \right] \left(\frac{\text{electrons}}{\text{unit area-unit energy-unit time}} \right)$$

where $H(x)$ is the unit step function, $H(x) = 1$ for $x \geq 0$, $H(x) = 0$ for $x < 0$.

For applications in which the electromagnetic response of a system is dominated by the more energetic electron emission components Equation (21) may be an adequate representation of the total emission current. In some cases, for example, in situations involving the exchange of charge between system components in close proximity, the charge imbalance and subsequent response may be significantly influenced by secondary electron emission.